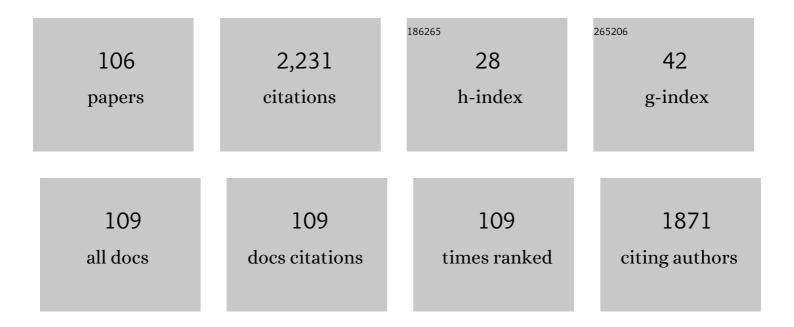
## Yoshihiko Ninomiya

List of Publications by Year in descending order

Source: https://exaly.com/author-pdf/4082813/publications.pdf Version: 2024-02-01



#	Article	IF	CITATIONS
1	Truly Transparent p-Type Î <sup>3</sup> -Cul Thin Films with High Hole Mobility. Chemistry of Materials, 2016, 28, 4971-4981.	6.7	166
2	Study on the species of heavy metals in MSW incineration fly ash and their leaching behavior. Fuel Processing Technology, 2016, 152, 108-115.	7.2	132
3	Influence of coal particle size on particulate matter emission and its chemical species produced during coal combustion. Fuel Processing Technology, 2004, 85, 1065-1088.	7.2	103
4	Emission of suspended PM from laboratory-scale coal combustion and its correlation with coal mineral properties. Fuel, 2006, 85, 194-203.	6.4	63
5	Highâ€Mobility Transparent pâ€Type Cul Semiconducting Layers Fabricated on Flexible Plastic Sheets: Toward Flexible Transparent Electronics. Advanced Electronic Materials, 2017, 3, 1700298.	5.1	62
6	Transformation of mineral and emission of particulate matters during co-combustion of coal with sewage sludge. Fuel, 2004, 83, 751-764.	6.4	61
7	Elucidating the mechanism of Cr(VI) formation upon the interaction with metal oxides during coal oxy-fuel combustion. Journal of Hazardous Materials, 2013, 261, 260-268.	12.4	53
8	CCSEM analysis of ash from combustion of coal added with limestone. Fuel, 2002, 81, 1499-1508.	6.4	50
9	Influence of woody biomass (cedar chip) addition on the emissions of PM10 from pulverised coal combustion. Fuel, 2011, 90, 77-86.	6.4	50
10	Effects of HCl, SO2 and H2O in flue gas on the condensation behavior of Pb and Cd vapors in the cooling section of municipal solid waste incineration. Proceedings of the Combustion Institute, 2011, 33, 2787-2793.	3.9	46
11	Fundamental Behaviors in Combustion of Raw Sewage Sludge. Energy & amp; Fuels, 2006, 20, 77-83.	5.1	45
12	Effect of Additives on the Reduction of PM <sub>2.5</sub> Emissions during Pulverized Coal Combustion <sup>â€</sup> . Energy & Fuels, 2009, 23, 3412-3417.	5.1	45
13	Use of Synchrotron XANES and Cr-Doped Coal to Further Confirm the Vaporization of Organically Bound Cr and the Formation of Chromium(VI) During Coal Oxy-Fuel Combustion. Environmental Science & Technology, 2012, 46, 3567-3573.	10.0	44
14	Synchrotron-Based XANES Speciation of Chromium in the Oxy-Fuel Fly Ash Collected from Lab-Scale Drop-Tube Furnace. Environmental Science & Technology, 2011, 45, 6640-6646.	10.0	43
15	Computer-Controlled Scanning Electron Microscopy (CCSEM) Investigation on the Heterogeneous Nature of Mineral Matter in Six Typical Chinese Coalsâ€. Energy & Fuels, 2007, 21, 468-476.	5.1	42
16	Transformation of phosphorus during combustion of coal and sewage sludge and its contributions to PM10. Proceedings of the Combustion Institute, 2007, 31, 2847-2854.	3.9	42
17	Theoretical study on the thermal decomposition of pyridine. Fuel, 2000, 79, 449-457.	6.4	41
18	Occurrence of Inorganic Elements in Condensed Volatile Matter Emitted from Coal Pyrolysis and Their Contributions to the Formation of Ultrafine Particulates during Coal Combustion. Energy & Fuels, 2006, 20, 1482-1489.	5.1	39

#	Article	IF	CITATIONS
19	Oxygen-Doped Zinc Nitride as a High-Mobility Nitride-Based Semiconductor. Journal of Physical Chemistry C, 2015, 119, 5327-5333.	3.1	38
20	<i>p</i> - to <i>n</i> -Type Conversion and Nonmetal–Metal Transition of Lithium-Inserted Cu <sub>3</sub> N Films. Chemistry of Materials, 2015, 27, 8076-8083.	6.7	35
21	Interactions among Inherent Minerals during Coal Combustion and Their Impacts on the Emission of PM10. 1. Emission of Micrometer-Sized Particles. Energy & Fuels, 2007, 21, 756-765.	5.1	34
22	Pilot-scale experimental and CFD modeling investigations of oxy-fuel combustion of Victorian brown coal. Fuel, 2015, 144, 111-120.	6.4	34
23	Conduction-band effective mass and bandgap of ZnSnN2 earth-abundant solar absorber. Scientific Reports, 2017, 7, 14987.	3.3	33
24	Effect of coal blending on the leaching characteristics of arsenic in fly ash from fluidized bed coal combustion. Fuel Processing Technology, 2013, 106, 769-775.	7.2	32
25	Effect of HCl, SO2 and H2O on the condensation of heavy metal vapors in flue gas cooling section. Fuel Processing Technology, 2013, 105, 181-187.	7.2	31
26	Ash partitioning during the oxy–fuel combustion of lignite and its dependence on the recirculation of flue gas impurities (H2O, HCl and SO2). Fuel, 2011, 90, 2207-2216.	6.4	30
27	Do FeCl3 and FeCl3/CaO conditioners change pyrolysis and incineration performances, emissions, and elemental fates of textile dyeing sludge?. Journal of Hazardous Materials, 2021, 413, 125334.	12.4	30
28	Effects of coal blending on the reduction of PM10 during high-temperature combustion 2. A coalescence-fragmentation model. Fuel, 2009, 88, 150-157.	6.4	28
29	Evaluation of a Mg-Based Additive for Particulate Matter (PM) <sub>2.5</sub> Reduction during Pulverized Coal Combustion <sup>â€</sup> . Energy & Fuels, 2010, 24, 199-204.	5.1	28
30	Comparative study of electron transport mechanisms in epitaxial and polycrystalline zinc nitride films. Journal of Applied Physics, 2016, 119, .	2.5	28
31	In situ desulfurization during combustion of high-sulfur coals added with sulfur capture sorbents. Fuel, 2003, 82, 255-266.	6.4	25
32	Effect of inorganic particulates on the condensation behavior of lead and zinc vapors upon flue gas cooling. Proceedings of the Combustion Institute, 2013, 34, 2821-2829.	3.9	25
33	A microscopic study of the precipitation of metallic iron in slag from iron-rich coal during high temperature gasification. Fuel, 2013, 103, 101-110.	6.4	24
34	Effect of magnesium additives on PM2.5 reduction during pulverized coal combustion. Fuel Processing Technology, 2013, 105, 188-194.	7.2	24
35	Combustibility of dried sewage sludge and its mineral transformation at different oxygen content in drop tube furnace. Fuel Processing Technology, 2004, 85, 983-1011.	7.2	23
36	Rheological evolution and crystallization response of molten coal ash slag at high temperatures. AICHE Journal, 2013, 59, 2726-2742.	3.6	23

#	Article	IF	CITATIONS
37	Mineral interactions and their impacts on the reduction of PM10 emissions during co-combustion of coal with sewage sludge. Proceedings of the Combustion Institute, 2009, 32, 2701-2708.	3.9	22
38	High-throughput optimization of near-infrared-transparent Mo-doped In2O3 thin films with high conductivity by combined use of atmospheric-pressure mist chemical-vapor deposition and sputtering. Thin Solid Films, 2017, 626, 46-54.	1.8	22
39	Characteristics of iron and sulphur in high-ash lignite (Pakistani lignite) and their influence on long-term T23 tube corrosion under super-critical coal-fired boiler conditions. Fuel, 2020, 264, 116855.	6.4	22
40	Interactions among Inherent Minerals during Coal Combustion and Their Impacts on the Emission of PM10. 2. Emission of Submicrometer-Sized Particles. Energy & Fuels, 2007, 21, 766-777.	5.1	21
41	Influence of gaseous SO2 and sulphate-bearing ash deposits on the high-temperature corrosion of heat exchanger tube during oxy-fuel combustion. Fuel Processing Technology, 2017, 167, 193-204.	7.2	21
42	An investigation on the heterogeneous nature of mineral matters in Assam (India) coal by CCSEM technique. Fuel Processing Technology, 2011, 92, 1068-1077.	7.2	20
43	Condensation Behavior of Heavy Metals during Oxy-fuel Combustion: Deposition, Species Distribution, and Their Particle Characteristics. Energy & amp; Fuels, 2013, 27, 5640-5652.	5.1	20
44	Experimental Investigation of the Combustion of Bituminous Coal in Air and O <sub>2</sub> /CO <sub>2</sub> Mixtures: 1. Particle Imaging of the Combustion of Coal and Char. Energy & Fuels, 2010, 24, 4803-4811.	5.1	19
45	Vaporization Mechanisms of Water-Insoluble Cs in Ash During Thermal Treatment with Calcium Chloride Addition. Environmental Science & Technology, 2016, 50, 13328-13334.	10.0	19
46	Role of CaCl 2 and MgCl 2 addition in the vaporization of water-insoluble cesium from incineration ash during thermal treatment. Chemical Engineering Journal, 2017, 323, 114-123.	12.7	19
47	Partitioning of sulfur and calcium during pyrolysis and combustion of high sulfur coals impregnated with calcium acetate as the desulfurization sorbent. Fuel, 2004, 83, 1039-1053.	6.4	18
48	Experimental investigation of the combustion of bituminous coal in air and O2/CO2 mixtures: 2. Variation of the transformation behaviour of mineral matter with bulk gas composition. Fuel, 2011, 90, 1361-1369.	6.4	18
49	Development of thermal spraying materials through several corrosion tests for heat exchanger tube of incinerators. Fuel Processing Technology, 2016, 141, 216-224.	7.2	18
50	Effect of Coal Drying on the Behavior of Inorganic Species during Victorian Brown Coal Pyrolysis and Combustion. Energy & Fuels, 2011, 25, 2764-2771.	5.1	16
51	Effect of silica additive on the high-temperature fireside tube corrosion during the air-firing and oxy-firing of lignite (Xinjiang coal) – Characteristics of bulk and cross-sectional surfaces for the tubes. Fuel, 2017, 187, 68-83.	6.4	16
52	Characteristics of slag, fly ash and deposited particles during melting of dewatered sewage sludge in a pilot plant. Journal of Environmental Management, 2006, 79, 163-172.	7.8	15
53	Coordination structures of organically bound paramagnetic metals in coal and their transformation upon solvent extraction. Fuel, 2008, 87, 2628-2640.	6.4	15
54	Evolution of organically bound metals during coal combustion in air and O2/CO2 mixtures: A case study of Victorian brown coal. Proceedings of the Combustion Institute, 2011, 33, 2795-2802.	3.9	15

#	Article	IF	CITATIONS
55	Ignitability and Combustibility of Yallourn Pyrolysis Char Blended with Pulverized Coal Injection Coal under Simulated Blast Furnace Conditions. Energy & Fuels, 2016, 30, 1858-1868.	5.1	15
56	Ignitability and combustibility of Yallourn pyrolysis char under simulated blast furnace conditions. Fuel Processing Technology, 2017, 156, 113-123.	7.2	14
57	Kinetic study of chlorine behavior in the waste incineration process. Proceedings of the Combustion Institute, 2009, 32, 335-342.	3.9	13
58	Effect of kaolin on ash partitioning during combustion of a low-rank coal in O2/CO2 atmosphere. Fuel, 2018, 222, 538-543.	6.4	13
59	Formation of Submicron Particulates (PM1) from the Oxygen-Enriched Combustion of Dried Sewage Sludge and Their Properties. Energy & amp; Fuels, 2007, 21, 88-98.	5.1	12
60	High-temperature tube corrosion upon the interaction with Victorian brown coal fly ash under the oxy-fuel combustion condition. Proceedings of the Combustion Institute, 2017, 36, 3941-3948.	3.9	12
61	Zinc nitride as a potential high-mobility transparent conductor. Physica Status Solidi (A) Applications and Materials Science, 2017, 214, 1600472.	1.8	11
62	Properties of water-soluble and insoluble particulate matter emitted from dewatered sewage sludge incineration in a pilot-scale ash melting furnace. Fuel, 2008, 87, 964-973.	6.4	10
63	Transparent conducting zinc nitride films. Japanese Journal of Applied Physics, 2014, 53, 05FX01.	1.5	10
64	Influence of Steam, Hydrogen Chloride, and Hydrogen Sulfide on the Release and Condensation of Zinc in Gasification. Industrial & Engineering Chemistry Research, 2016, 55, 6911-6921.	3.7	10
65	Occurrence and characteristics of abundant fine included mineral particles in Collie coal of Western Australia. Fuel, 2018, 216, 53-60.	6.4	10
66	Characterization of combustionâ€derived individual fine particulates by computerâ€controlled scanning electron microscopy. AICHE Journal, 2009, 55, 3005-3016.	3.6	9
67	Effect of the optimal combination of bituminous coal with high biomass content on particulate matter (PM) emissions during co-firing. Fuel, 2022, 316, 123244.	6.4	9
68	Fate of Alkali Elements during Pyrolysis and Combustion of Chinese Coals Journal of Chemical Engineering of Japan, 2003, 36, 759-768.	0.6	8
69	Combustion and De–SOx behavior of high-sulfur coals added with calcium acetate produced from biomass pyroligneous acid. Fuel, 2004, 83, 2123-2131.	6.4	8
70	Effect of HCl/SO2/H2O on the Deposition of Heavy Metal Vapors in the Cooling Section of an Incineration Plant. Journal of Chemical Engineering of Japan, 2010, 43, 713-719.	0.6	6
71	Effect of H2S concentration in gasified gas on the microstructure and leaching properties of coal slag. Fuel, 2014, 116, 812-819.	6.4	6
72	Vaporization Behavior of Cs, K, and Na in Cs-Containing Incineration Bottom Ash during Thermal Treatment with CaCl <sub>2</sub> and CaO. Energy & Fuels, 2017, 31, 14045-14052.	5.1	6

#	Article	IF	CITATIONS
73	Enhancement of Cs vaporization from simulated granular ash through thermal treatment in N2 atmosphere with the addition of a mixture of CaCl2 and CaO. Fuel, 2018, 214, 409-415.	6.4	6
74	Low-temperature trace light-tar reforming in biomass syngas by atmospheric hydrogenation and hydrogenolysis. Fuel Processing Technology, 2018, 181, 304-310.	7.2	6
75	Use of thermal treatment with CaCl2 and CaO to remove 137Cs in the soil collected from the area near the Fukushima Daiichi Nuclear Power Plant. Journal of Hazardous Materials, 2021, 401, 123364.	12.4	6
76	Influence of Steam, Hydrogen Chloride, and Hydrogen Sulfide on the Release and Condensation of Cadmium in Gasification. Energy & Fuels, 2016, , .	5.1	5
77	The effect of ceria content in nickel–ceria composite anode catalysts on the discharge performance for solid oxide fuel cells. International Journal of Hydrogen Energy, 2018, 43, 2394-2401.	7.1	4
78	Selective Synthesis of the Iminophosphoranes and Phosphorus Ylides from (Alkylamino)phosphonium Salts. Comparative Study of Electrochemical Reduction with the Base Method. Electrochemistry, 2005, 73, 798-806.	1.4	3
79	Elution of Ti during solvent extraction of coal and the transformation of eluted Ti upon combustion. AICHE Journal, 2008, 54, 1646-1655.	3.6	3
80	Synergistic Mechanisms of CaCl <sub>2</sub> and CaO on the Vaporization of Cs from Cs-Doped Ash during Thermal Treatment. Energy & Fuels, 2018, 32, 5433-5442.	5.1	3
81	Partitioning of Lead and Lead Compounds under Gasification-Like Conditions. Energy & Fuels, 2018, 32, 651-657.	5.1	3
82	Influence of Inherent Moisture on the Formation of Particulate Matter during Low-Rank Coal Combustion. Journal of Chemical Engineering of Japan, 2017, 50, 351-357.	0.6	3
83	Behavior of Chlorine in HCl/H2O/O2/CO2/N2 Reaction System. Journal of Chemical Engineering of Japan, 2008, 41, 519-524.	0.6	2
84	Effects of Mineral Transformations on the Reduction of PM <sub>2.5</sub> during the Combustion of Coal Blends. Advanced Materials Research, 0, 356-360, 1306-1314.	0.3	2
85	Current Issues of Ash Deposition and Corrosion on Waste-to-Energy Plant. Nihon Enerugi Gakkaishi/Journal of the Japan Institute of Energy, 2016, 95, 1089-1104.	0.2	2
86	Ni-CeO <sub>2</sub> Nano-composite Anode for Solid Oxide Fuel Cell with ScSZ Electrolyte for Biomass Gasification Fuel Cell Power Generation System. Nihon Enerugi Gakkaishi/Journal of the Japan Institute of Energy, 2016, 95, 922-929.	0.2	2
87	Spatial distribution of chromium on the corroded tube surface characterised by synchrotron X-ray fluorescence (SXRF) mapping and μ-XANES: Co-existence of Ca-rich ash deposits and oxy-firing flue gas. Fuel Processing Technology, 2017, 167, 31-42.	7.2	2
88	Reaction mechanisms underpinning the removal of Cs from simulated Cs-contaminated ash during thermal treatment with NaCl or KCl. Fuel, 2021, 289, 119905.	6.4	2
89	Clinker Formation Behavior in a Co-current Up-flowing Moving Bed Gasifier Fueled with Japanese Cedar Pellets. Nihon Enerugi Gakkaishi/Journal of the Japan Institute of Energy, 2021, 100, 236-244.	0.2	2
90	Kinetic Study of Long-Term T23 Tube Corrosion upon Low-Rank Coal Ash Deposition under Oxy-Fuel Combustion Conditions. Energy & Fuels, 2019, 33, 10209-10217.	5.1	1

#	Article	IF	CITATIONS
91	Sintering Behavior of Coal Ash Build Up on Ceramic Filters in a Hot Gas Filtration System. , 2003, , .		1
92	Oxidation Reaction of Calcium Sulfide in an Advanced PFBC Condition. (II). Sulfation Reaction and Grain Model Application Nihon Enerugi Gakkaishi/Journal of the Japan Institute of Energy, 1999, 78, 750-759.	0.2	1
93	Analysis of Coal Ash Build up on Ceramic Filters in a Hot Gas Filtration System. Nihon Enerugi Gakkaishi/Journal of the Japan Institute of Energy, 2005, 84, 359-365.	0.2	1
94	Effect of Aluminum Oxide Additives for Suppressing Clinker Formation in a Co-current Up-flowing Moving Bed Gasifier Fueled by Japanese Cedar Pellets. Nihon Enerugi Gakkaishi/Journal of the Japan Institute of Energy, 2021, 100, 245-253.	0.2	1
95	Nonlinear Phenomena. Effects of Temperature, O2 Partial Pressure, Initial CaS Content and Particle Diameter on Oxidation Reaction of CaS Particles Kagaku Kogaku Ronbunshu, 1999, 25, 635-641.	0.3	0
96	Correlation Analyses between the Mobilities on Paper Electrophoresis of Alkysubstituted Phosphonium Ions (RR <sub>3</sub> ′P <sup>+</sup> ). Nippon Kagaku Kaishi / Chemical Society of Japan - Chemistry and Industrial Chemistry Journal, 2001, 2001, 91-95.	0.1	0
97	Investigation of a direct melting dehydrated sewage sludge pilot plant. International Journal of Environment and Pollution, 2007, 31, 371.	0.2	0
98	Condensation Behavior of Heavy Metal Vapors upon Flue Gas Cooling in Oxy-fuel versus Air Combustion. Journal of Chemical Engineering of Japan, 2015, 48, 450-457.	0.6	0
99	Spatial distribution of Cr-bearing species on the corroded tube surface characterised by synchrotron X-ray fluorescence (SXRF) mapping and micro-XANES: exposure of tubes in oxy-firing flue gas. Journal of Materials Science, 2018, 53, 11791-11812.	3.7	0
100	Sintering Behavior of Coal Ash Build up on Ceramic Filters in a Hot Gas Filtration System. Nihon Enerugi Gakkaishi/Journal of the Japan Institute of Energy, 2005, 84, 767-772.	0.2	0
101	石ç,燃焼ã•ã,‰æŽ'出ã•ã,Œã,‹ç²'åçŠ¶å¾®é‡æœ‰å®³ç‰©è³ªã®æŒ™å‹•解枕 Hosokawa Powder Techr	io <b>logy</b> Fou	Indation AN
102	Evaluation of nanosized additives for environmental pollutant reduction during solid fuel combustion. Hosokawa Powder Technology Foundation ANNUAL REPORT, 2009, 17, 37-42.	0.0	0
103	Influence of Ni-CeO <sub>2</sub> composition as anode catalyst in a SOFC on discharge performance. The Proceedings of the National Symposium on Power and Energy Systems, 2017, 2017.22, D131.	0.0	0
104	Influence of methane fuel on terminal voltage of a Ni-GDC anode electrode. The Proceedings of the National Symposium on Power and Energy Systems, 2018, 2018.23, C121.	0.0	0
105	Prediction of ash-deposition characteristics in co-combustion conditions with CCSEM. The Proceedings of the International Conference on Power Engineering (ICOPE), 2021, 2021.15, 2021-0129.	0.0	0
106	Prediction method of ash deposition based on combustion state of solid fuel. Mechanical Engineering Journal, 2022, , .	0.4	0